

Carbide-Derived Nanoporous Carbon and Novel Core–Shell Nanowires

Xinqi Chen,[†] Donald R. Cantrell,[†] Kevin Kohlhaas,[†] Sasha Stankovich,[†] James A. Ibers,[‡] Mietek Jaroniec,[§] Hongsheng Gao,[⊥] Xiaodong Li,[⊥] and Rodney S. Ruoff^{*,†}

Departments of Mechanical Engineering and Chemistry, Northwestern University, Evanston, Illinois 60208, Department of Chemistry, Kent State University, Kent, Ohio 44242, and Department of Mechanical Engineering, University of South Carolina, Columbia, South Carolina 29208

Received September 2, 2005. Revised Manuscript Received November 29, 2005

Carbide-derived carbon (CDC) nanowires (NWs) have been synthesized by the high-temperature treatment of small-diameter β -SiC whiskers with Cl_2/H_2 . A variety of physical measurements indicate that Si was extracted by exposure to Cl_2 and that the C in the carbon nanowires is primarily sp^2 -bonded. From BET measurements, the specific surface area of these carbon nanowires is $1.3 \times 10^3 \text{ m}^2/\text{g}$ and they contain a network of nanopores. Nanoindentation measurements indicate that the SiC-derived C is not a stiff material, the elastic modulus being $5.0 \pm 1.2 \text{ GPa}$. High-temperature treatment of the CDC nanowires under an inert gas significantly increases the degree of graphitization. In addition, partial extraction was used to obtain core–shell structures having a thin and also very high surface area CDC shell; further treatment at high temperature was used to produce graphitized carbon shell–crystalline SiC core NWs.

Introduction

Carbon materials, such as diamond, graphite, and amorphous carbon, are of interest because of their physical and chemical properties. Gogotsi et al.¹ reported the synthesis of nano- and microcrystalline diamond-structured carbon films by extraction of the Si from the surface region of macroscopic SiC samples with Cl_2 -containing gases at ambient pressure and temperatures not exceeding $1000 \text{ }^\circ\text{C}$. This method to produce “carbide-derived carbon (CDC)” has been used for the conversion of the surface layer of macroscopic samples of silicon carbide to nanocrystalline diamond, graphite, and amorphous carbon films on SiC.^{1–5} In further work it was found that the CDC material possesses a microporous structure and that the distribution of pore sizes is tunable by adjustment of the reaction temperature.^{6,7} So far, SiC precursors of both bulk and particulate forms have been investigated. However, the study of CDC materials and the methods for their production are still incomplete.

Carbon films can be obtained by the metal extraction of metal carbides by halogens. In this process, metal is extracted preferentially by the halogen, and elemental carbon is left behind. The most extensively studied system of this type is the Cl_2/SiC system in which Si is removed from SiC in the form of SiCl_4 by the following reaction:⁵



The corresponding reaction for the removal of C as CCl_4 is much less thermodynamically favorable.



The structure of the remaining carbon can vary, depending on parameters of the reaction such as temperature, duration, and the presence and concentration of H_2 . It has been reported that when H_2 is added to the Cl_2/SiC system, it can stabilize dangling sp^3 bonds in the CDC samples.⁵ Additionally, H_2 might react with the Cl_2 to form HCl. HCl (whether created by the reaction of H_2 with Cl_2 or introduced to the system as a precursor gas) can react with SiC to create CDC material primarily by the following reaction, which has a much smaller thermodynamic driving force than the reactions for Si removal by Cl_2 :⁵



The objectives of the present study are the synthesis and characterization of nanoporous carbon nanowires and SiC core–carbon shell nanowires by the extraction of Si with Cl_2/H_2 mixtures from small-diameter SiC whiskers.

Experimental Section

Synthesis. The β -SiC whiskers used as the precursor were obtained from Advanced Composite Materials Corp., SC. They have

* Correspondence should be addressed to r-ruoff@northwestern.edu, 1-847-467-6596 (phone).

[†] Department of Mechanical Engineering, Northwestern University.

[‡] Department of Chemistry, Northwestern University.

[§] Kent State University.

[⊥] University of South Carolina.

(1) Gogotsi, Y.; Welz, S.; Ersoy, D. A.; McNallan, M. J. *Nature (London, U. K.)* **2001**, *411*, 283–287.

(2) Nikitin, A.; Gogotsi, Y. *Encycl. Nanosci. Nanotechnol.* **2004**, *7*, 553–574.

(3) Hoffman, E. N.; Yushin, G.; Barsoum, M. W.; Gogotsi, Y. *Chem. Mater.* **2005**, *17*, 2317–2322.

(4) Dimovski, S.; Nikitin, A.; Ye, H.; Gogotsi, Y. *J. Mater. Chem.* **2004**, *14*, 238–243.

(5) Gogotsi, Y. G.; Jeon, I.-D.; McNallan, M. J. *J. Mater. Chem.* **1997**, *7*, 1841–1848.

(6) Dash, R. K.; Nikitin, A.; Gogotsi, Y. *Microporous Mesoporous Mater.* **2004**, *72*, 203–208.

(7) Gogotsi, Y.; Nikitin, A.; Ye, H.; Zhou, W.; Fischer, J. E.; Yi, B.; Foley, H. C.; Barsoum, M. W. *Nat. Mater.* **2003**, *2*, 591–594.

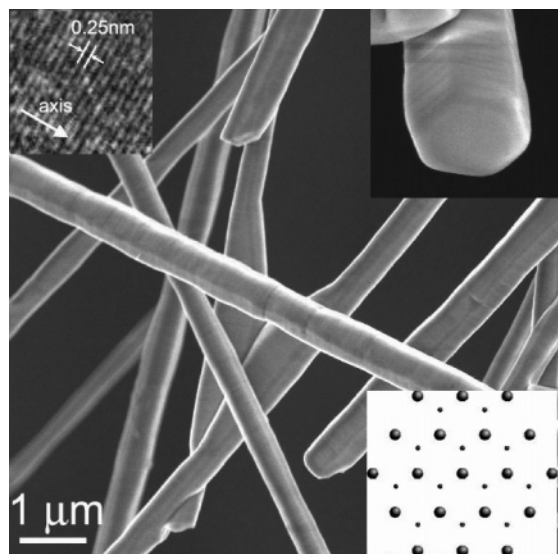


Figure 1. SEM image of β -SiC whiskers on a Cu TEM grid. Upper right inset: SEM image of a β -SiC whisker shows it has a hexagonal end and faceted sides. Lower inset: lattice structure of the (111) plane. Upper left inset: TEM image shows the [111] direction along the axis.

a quoted purity of 99% with diameters in the range of 0.45–0.65 μm and lengths in the range of 5–80 μm . Scanning electron microscopy (SEM) and transmission electron microscopy (TEM) images of the precursor material are shown in Figure 1. The hexagonal ends and the facets of the β -SiC crystals are visible from the SEM image, and the lattice structure of the (111) plane is also illustrated in the lower right inset of Figure 1. The TEM image shown in the upper left inset indicates that the SiC whisker grew along the [111] direction.

The silicon extraction experiments have been carried out in a home-built thermal chemical vapor deposition (CVD) apparatus that was set in a chemical hood. The light green β -SiC powder was loaded into a fused silica tube that was inserted into a horizontal tube furnace. The tube was purged with Ar (20 standard cubic centimeters, (scm), BOC Gases, 99.999%) for 1 h, followed by heating to the desired temperature at the rate of 16 $^{\circ}\text{C}/\text{min}$. Once the desired temperature was achieved, the Ar flow was stopped and the desired ratio of $\text{Cl}_2:\text{H}_2$ was introduced at a rate of 20–30 sccm. Both the Cl_2 and H_2 precursor gases were diluted with Ar to achieve concentrations of 3.5% and 5%, respectively, by Matheson Tri-gas. The mixture of gases was passed through anhydrous Drierite (97 wt % CaSO_4 and 3 wt % CoCl_2 from W. A. Hammond Drierite Co. Ltd., Xenia, OH) and a sulfuric acid bubbler to remove any water that might have been present as a contaminant. After several hours of maintaining the chamber at an elevated temperature, the sample was cooled under Ar(g). A bubbler containing NaOH solution was attached to the exhaust tubing to consume the remaining Cl_2 .

Characterization. The color of the powdered product was observed to be black, gray, or light green, depending on the extent of the reaction. The samples were suspended in absolute ethanol and sonicated for 1 h. A few drops of the suspension were placed on lacey carbon TEM grids (Ted Pella, Inc., CA) that were used for characterization by TEM (Hitachi HF2000), SEM (Leo 1525), energy dispersive X-ray spectroscopy (EDX, Oxford Instruments INCA 4.05 on the Hitachi HF2000 TEM), and electron energy loss spectroscopy (EELS, Gatan Image Filter Digital Micrograph 3.6 on the Hitachi HF2000 TEM).

The nitrogen adsorption isotherm for the sample studied was measured at $-195.8\text{ }^{\circ}\text{C}$ by using a Micromeritics ASAP 2010 accelerated surface area and porosimetry analyzer. Prior to the

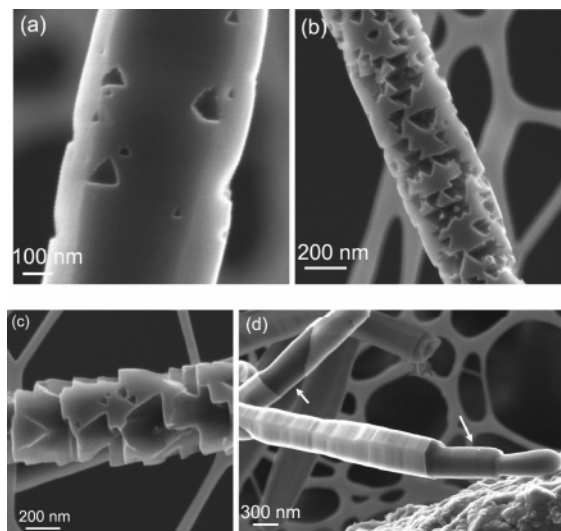


Figure 2. SEM images of the CDC NWs. (a–c) The sample reacted at 1000 $^{\circ}\text{C}$ for 10 h with $\text{Cl}_2:\text{H}_2 = 1:0.5$. (d) The sample reacted at 950 $^{\circ}\text{C}$ for 6.5 h with $\text{Cl}_2:\text{H}_2 = 1:0.7$. (White arrows: converted to C).

analysis, the powder was outgassed at 200 $^{\circ}\text{C}$ for 3 h under vacuum. The specific surface area of the powder was evaluated according to the BET (Brunauer, Emmett, and Teller) method using adsorption data in the range of relative pressures from 0.01 to 0.15. The single-point pore volume was estimated from the amount adsorbed at a relative pressure of about 0.99. The entire adsorption branch of the isotherm was used to calculate the pore size distribution (PSD) by using the DFT (density functional theory) Plus software (Micromeritics, Inc.) elaborated for slitlike pores, which employs the regularization method to invert the adsorption integral equation with respect to the PSD. From a numerical viewpoint, this inversion requires the solution of a system of linear equations that contains the matrix of local isotherms representing adsorption in single pores of different sizes generated by nonlocal DFT.^{8,9}

A Hysitron Triboscope nanoindenter in conjunction with a Veeco Dimension 3100 AFM was used for nanoindentation tests. A Berkovich diamond nanoindenter tip was used to locate a CDC NW synthesized at 1000 $^{\circ}\text{C}$ for 9 h with only Cl_2 , and the indenter tip was positioned on the CDC NW to perform an indentation test in-situ. The nanoindenter monitored and recorded the load and displacement of a three-sided pyramidal diamond (Berkovich) indenter during indentation with a force resolution of ~ 1 nN and a displacement resolution of ~ 0.2 nm.^{10,11} Hardness and elastic modulus were calculated from the load-displacement data obtained by nanoindentation.

Results and Discussion

Owing to the large quantity of the β -SiC whisker sample, it is evident that the reaction did not occur on all of the NWs at the same rate. For reactions of short duration, the color of the top layer of the sample was converted to black whereas the bottom remained light green, suggesting that the bottom of the sample did not react. Figure 2 shows SEM images of β -SiC whisker samples treated at two different conditions. Parts a–c of Figure 2 show the sample reacted at 1000 $^{\circ}\text{C}$ for 10 h with $\text{Cl}_2:\text{H}_2 = 1:0.5$ that was fully reacted; part d shows the sample reacted at 950 $^{\circ}\text{C}$ for 6.5 h with $\text{Cl}_2:\text{H}_2 = 1:0.7$ that was partially reacted. The SEM images show that

(8) Olivier, J. P. *Carbon* **1998**, *36*, 1469–1472.

(9) Olivier, J. P. *Stud. Surf. Sci. Catal.* **2004**, *149*, 1–33.

(10) Bhushan, B.; Li, X. *Int. Mater. Rev.* **2003**, *48*, 125–164.

(11) Li, X.; Bhushan, B. *Mater. Charact.* **2002**, *48*, 11–36.

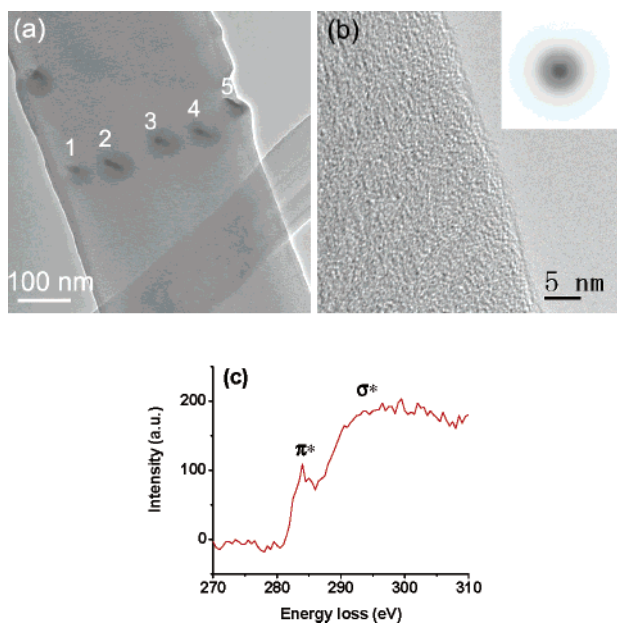


Figure 3. (a) Low-magnification TEM image and (b) high-magnification TEM image of the CDC NW, inset: electron diffraction on the CDC NW; (c) EELS spectrum taken with the Hitachi HF-2000 at the edge of the CDC NW.

Table 1. Atomic Percentages for the Five Spots Shown in Figure 3a^a

spot	C	Si	O	Cl
1	97.5	0.3	0.8	0.5
2	97.3	0.2	0.9	0.8
3	97.2	0.2	0.9	0.9
4	97.3	0.3	0.9	0.6
5	98.3	0.6	0	0

^a Oxford Instruments INCA 4.05 (EDX software).

many trigonal etch pits were formed on the surface of the β -SiC whiskers. Because β -SiC can be distinguished from α -SiC by its trigonal etch pits,¹² their presence confirms that the SiC whiskers are β -SiC (as was already known). On the basis of defect-selective wet etching with KOH of β -SiC, these etch pits probably correspond to the dislocations that are associated with closely spaced parallel {111} stacking faults.

TEM images of the CDC NWs are shown in Figure 3a,b. The Si-extraction for this sample was carried out at 1000 °C for 7 h with $\text{Cl}_2:\text{H}_2 = 1:0.5$. The high-resolution TEM image and electron diffraction data (inset) indicate that the structure is amorphous. EDX analysis was performed on this CDC NW, and the data are given in Table 1. The material is nearly pure C (for the elements that can be detected by EDX, which does not include H) with no significant variation of the composition across the specimen.

EELS was used to determine the C $\text{sp}^2:\text{sp}^3$ ratio, specifically for CDC NWs treated at 1000 °C for 7 h with $\text{Cl}_2:\text{H}_2 = 1:0.5$. To determine the fraction of sp^2 -bonded C atoms, the EELS spectra (shown in Figure 3c) were analyzed by the method proposed by Cuomo et al.¹³ A graphite sample (HOPG; ZYB grade, SPI-2, SPI Inc.) was used as a reference for pure sp^2 bonding in the EELS analysis. The integrated

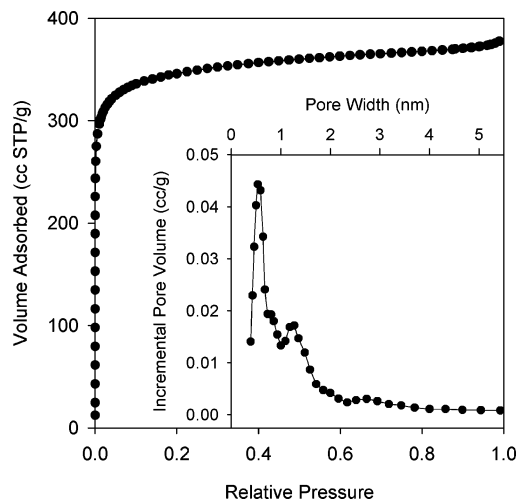


Figure 4. Nitrogen adsorption isotherm and the corresponding pore size distribution (see inset).

intensity in the range from 290 to 305 eV is contributed by the excitation from the ground-state core 1s to the σ^* state; the intensity in the range from 284 to 289 eV is contributed by the excitation to the π^* state. The fraction of the sp^2 -bonded C was found to be ~ 0.88 . Thus sp^2 bonding dominates the structure of these CDC NWs.

Adsorption Properties of CDC NWs. The surface area and pore size of these CDC NWs were measured, both for fundamental interest and because materials with high specific surface area and controlled pore size distribution have potential applications as molecular sieves, gas storage structures, catalysts, absorbents, and water/air filters. Two samples treated at 1000 °C for 10 h with $\text{Cl}_2:\text{H}_2 = 1:0.5$ have been analyzed. The nitrogen adsorption isotherm was recorded at -195.8 °C, and the data are shown in Figure 4. This is a typical type I isotherm according to the IUPAC classification; it is characteristic of highly microporous solids, i.e., solids possessing a large fraction of fine pores with widths below 2 nm.^{14,15} The single-point pore volume estimated from the amount adsorbed at the relative pressure of about 0.99 is $0.58 \text{ cm}^3/\text{g}$, confirming the high porosity of these CDC NWs. The BET surface area of this sample, evaluated by using adsorption data in the range of relative pressures from 0.01 to 0.15, is $1.3 \times 10^3 \text{ m}^2/\text{g}$. The pore size distribution for this sample is shown in the inset of Figure 4. Analysis of this distribution shows that 94% of the total pore volume is due to micropores, i.e., pores below 2 nm in diameter, 4% is due to pores between 2 and 4 nm, and only 2% is due to pores with diameters greater than 4 nm. Adsorption analysis of another sample prepared under the same conditions gave analogous parameters. (Here, we use the terminology of the adsorption measurement field; clearly “microporous”, in these CDC NW samples, is indicative of extremely small diameter nanopores, as mentioned above.)

Mechanical Properties. Figure 5 shows the load-displacement curve of an indentation made at an 80 μN peak

(12) Zhuang, D.; Edgar, J. H. *Mater. Sci. Eng., R: Reports R* **2005**, *48*, 1–46.

(13) Cuomo, J. J.; Doyle, J. P.; Bruley, J.; Liu, J. C. *Appl. Phys. Lett.* **1991**, *58*, 466–468.

(14) Kruk, M.; Jaroniec, M. *Chem. Mater.* **2001**, *13*, 3169–3183.

(15) Sing, K. S. W.; Everett, D. H.; Haul, R. A. W.; Moscou, L.; Pierotti, R. A.; Rouquerol, J.; Siemieniewska, T. *Pure Appl. Chem.* **1985**, *57*, 603–619.

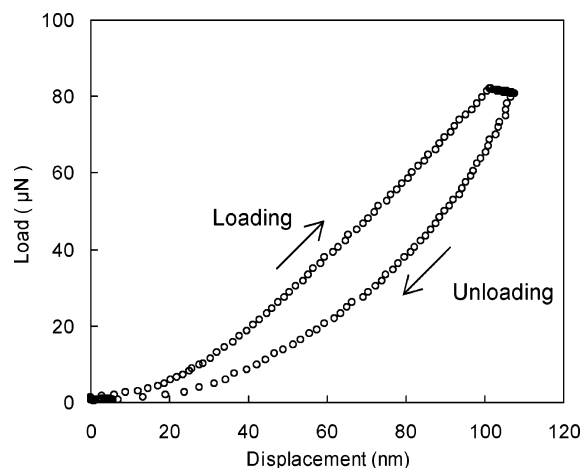


Figure 5. Typical load-displacement curve from an indentation test on an individual CDC NW.

indentation load on an individual CDC NW. The nanoindentation unloading curve has an elbow, almost complete recovery after unloading and the full curve shows hysteresis. The unloading elbow event has been found in both amorphous and crystalline materials, such as Si, Ge, diamond, InP, and quartz.^{10,11,16} It is believed that the elbow in the unloading curve is a result of material expansion during phase transformation from amorphous carbon to crystalline carbon.¹⁶ The Poisson's ratio¹⁷ for amorphous carbon of 0.25 ± 0.05 was used to calculate the hardness and elastic modulus of 0.58 ± 0.18 GPa and 5.0 ± 1.2 GPa, respectively, from these data. This elastic modulus is substantially lower than the lowest value (~ 100 GPa) for hydrogenated amorphous carbon (α -C:H), as modeled by Tersoff.¹⁸ However, Tersoff modeled α -C:H with nearly ideal sp^3 bonding. Amorphous hydrogenated carbon films contain a mixture of sp^2 - and sp^3 -bonded C atoms. When the sp^2 content is high, as is the case for the Si-extracted CDC NWs studied here, one expects a lower elastic modulus and hardness. Additionally, there exists a high density of nanopores in these samples, and these would significantly decrease the hardness and elastic modulus of the material. The hardness:elastic modulus ratio, $H:E = 0.12$, is consistent with results on other α -C:H films.¹⁹

Effects of $Cl_2:H_2$. To determine the role of H_2 in the reaction, we have changed $Cl_2:H_2$ in the gas mixture from 1:0 to 1:1.86 while maintaining the other parameters constant. All of these CVD reactions were carried out at 1000 °C for 10 h for a similar amount of precursor. Although the structure of the individual NWs could be determined by TEM measurements, it was difficult to obtain an overall estimation of the extent of the reaction because of its strong dependence on the location of the precursor in the quartz boat. A qualitative estimation could be made from the color change in the sample: the precursor was green, the fully Si-extracted

sample was black, and the partially Si-extracted sample was an intermediate in color depending on the extent of the reaction. We conclude that the reaction became slower as the H_2 concentration was increased and ceased when $Cl_2:H_2 < 1$.

Although it has been reported⁵ that the addition of H_2 to a chlorination reaction stabilizes dangling bonds and increases sp^3 bonding, this did not occur in the experiments reported here. For $Cl_2:H_2$ of 1:0, 1:0.5, 1:0.66, and 1:0.74, Si extraction reached completion in the reactions run at 1000 °C for 10 h. The TEM images recorded from these samples indicated similar amorphous structures, and the EELS results showed that all of the samples had a fraction of sp^2 -bonded C of ~ 0.8 – 0.9 . When $Cl_2:H_2$ was 1:0.83, the Si-extraction was only partially completed and the color of the sample was gray. When the ratio of $Cl_2:H_2$ was changed to 1:1 and 1:1.86, the Si-extraction did not occur to any appreciable extent and the color of the sample remained that of the precursor. Probably HCl formed in these last two gas mixtures; it is not effective at removing Si (eq 3). Thus, we find that the addition of H_2 only affects the reaction rate but does not affect the bonding character of the carbide-derived carbon.

Core–Shell Nanostructure. When the SiC whiskers have been treated at 800 °C for a short time with a $Cl_2:H_2 = 1:0.5$, only a thin layer of SiC was converted to amorphous C. The thicknesses of the carbon layers of the 1 h treated sample and 3 h treated sample were 8.3 ± 2.8 nm and 28 ± 14 nm, respectively. The low magnification TEM images of these partially extracted SiC whiskers are shown in Figure 6. The 1 h treated sample still had a smooth surface. However, the 3 h treated sample had a rough surface, and many etch pits formed. BET surface area measurements have been conducted on these two samples and also on the precursor β -SiC whiskers. The BET surface areas were 24 m²/g (1 h treated sample), 70 m²/g (3 h treated sample), and 4 m²/g for the β -SiC whiskers. No porous structure was found in the precursor β -SiC whiskers. With some reasonable assumptions, it is possible to assign specific surface areas to the 1 h and 3 h treated samples. We assume that the SiC cores are fully covered by the carbon shell layers. The density of bulk β -SiC is 3.21 g/cm³, and this is assumed for the SiC whisker core. The amorphous carbon in the shell is assumed to have a density of 2.0 g/cm³.²⁰ The mean diameter of the core–shell NWs is assumed to be identical to that of the precursor sample, $(5.8 \pm 1.3) \times 10^2$ nm (34 whiskers measured). With these assumptions, the carbon shell layer specific surface areas are 1.3×10^3 m²/g (1 h treated sample) and 1.1×10^3 m²/g (3 h-treated sample). These BET results are reasonably consistent with those for the fully Si-extracted samples. Whereas nitrogen adsorption isotherms without hysteresis were measured for the fully Si-extracted samples (see Figure 4), small hysteresis loops were observed on the isotherms for the 1 h treated and 3 h treated samples (not shown), which indicate a gradual development of nanoporous carbon layers and the formation of novel SiC core–nanoporous carbon NWs.

(16) Gogotsi, Y.; Domnich, V. *High-Pressure Surface Science and Engineering: Series in Materials Science and Engineering*; Institute of Physics Publishing: Philadelphia, PA, 2003; p 639.

(17) Marques, F. C.; Lacerda, R. G.; Champi, A.; Stolojan, V.; Cox, D. C.; Silva, S. R. P. *Appl. Phys. Lett.* **2003**, *83*, 3099–3101.

(18) Tersoff, J. *Phys. Rev. B: Condens. Matter.* **1991**, *44*, 12039–12042.

(19) Robertson, J. *Phys. Rev. Lett.* **1992**, *68*, 220–223.

(20) Cardarelli, F. *Materials Handbook: A Concise Desktop Reference*; Springer: London, 2000.

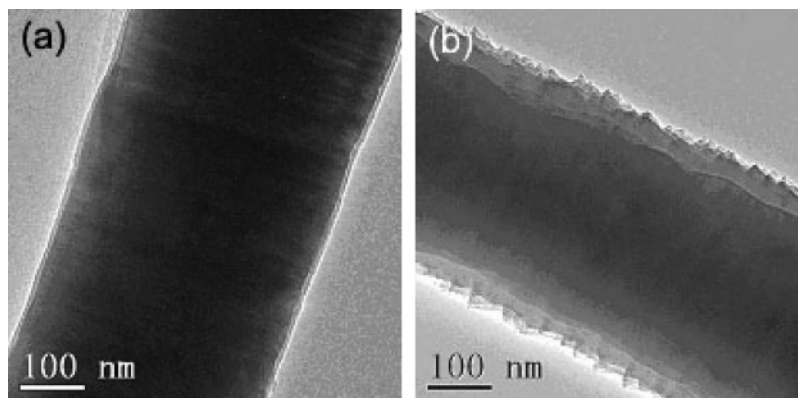


Figure 6. Low-magnification TEM images of the partially extracted SiC whiskers: (a) treated at 800 °C for 1 h with a Cl₂:H₂ ratio of 1:0.5; (b) treated at 800 °C for 3 h with a Cl₂:H₂ ratio of 1:0.5.

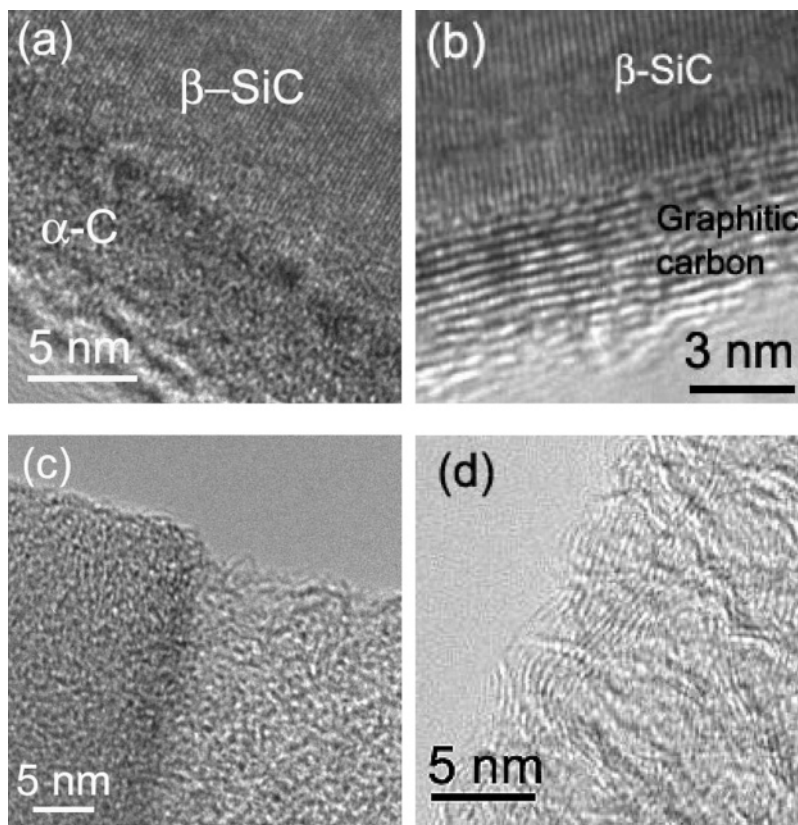


Figure 7. TEM images of the CDC NWs before and after annealing at 2000 °C: (a) before annealing and (b) after annealing a partially-Si-extracted sample for 1 h; (c) before annealing and (d) after annealing a fully-Si-extracted sample for 2 h.

The 1 h treated sample as well as a fully Si-extracted sample were subjected to an annealing temperature of 2000 °C in an Ar environment with a gauge pressure of 360 Torr. The TEM images (Figure 7a,b) show that the amorphous carbon outer shell on the partially extracted sample had been converted to graphitized carbon after 1 h high-temperature treatment. We have also treated the precursor SiC whiskers under the same conditions and find that the outer layer of SiC decomposed and converted to a graphitic layer. This is consistent with a previous report.²¹ Therefore, we believe that the graphitic carbon layers in Figure 7b partially arose from the decomposition of SiC and partially from the graphitization of amorphous carbon.

The fully extracted sample was treated at the high temperature for 2 h. The TEM image (Figure 7d) shows an easily observed but smaller graphitic carbon region compared to the amorphous structure that the sample had prior to the treatment (Figure 7c).

This novel material with a graphitized carbon shell and a crystalline SiC core structure may have potential applications in electronics as it is likely that the shell is highly conductive and the core is semiconducting.

Summary

We have converted β -SiC whiskers to carbon NWs by the carbide-derived carbon (CDC) method. The CDC NWs have an sp²-bond-rich amorphous structure. These carbon NWs have a specific surface area of 1.3×10^3 m²/g and a large concentration of nanopores with diameters less than 2 nm.

(21) Cambaz, Z. G.; Yushin, G. N.; Gogotsi, Y. *J. Am. Ceram. Soc.* **2005**, in press. <http://www.blackwell-synergy.com/doi/abs/10.1111/j.1551-2916.2005.00780.x?prevSearch=allfield%3A%28gogotsi%29>.

The hardness and elastic modulus of the NWs were 0.58 ± 0.18 GPa and 5.0 ± 1.2 GPa, respectively; these low values are believed to be due to the sp^2 bonding and porous structure. We conclude that the simultaneous addition of H_2 adjusts only the reaction rate; it does not significantly increase the sp^3 bonding in the carbon NWs. Novel core-shell NWs were created by partial extraction, and the carbide-derived carbon shells surrounding the β -SiC core have very high specific surface area, suggesting use as chemical sensors. High-temperature treatment markedly increases the degree of graphitization, and by this process we also produced novel SiC core-graphitized carbon shell nanostructures. Because of the large-scale availability (ton level) of the β -SiC whiskers, these novel core shell structures are likely to find use in a host of applications, from the aforementioned sensor possibilities to their incorporation in composites.

Acknowledgment. We appreciate partial support from a grant administered through the Naval Research Laboratory (Nanofilament-Based Combined C/B Detectors; N00173-04-2-C003/ P00003) and also from NASA (Award NCC-1-02037) through the University Research, Engineering, and Technology Institute on Bio-inspired Materials (BiMat). The SEM, TEM, EDX, and EELS measurements were performed in the EPIC facility of the NUANCE Center at Northwestern University. The NUANCE Center is supported by NSF-NSEC, NSF-MRSEC, Keck Foundation, the State of Illinois, and Northwestern University. H. G. and X. L. were supported by the National Science Foundation (Grant No. EPS-0296165) and a University of South Carolina NanoCenter Seed Grant.

CM051991O